Ultramicroscopy 108 (2008) 1128–1134

Contents lists available at ScienceDirect

Ultramicroscopy

journal homepage: www.elsevier.com/locate/ultramic

Atomic force microscopy study of the antibacterial effects of chitosans on *Escherichia coli* and *Staphylococcus aureus*

Peter Eaton [a,*], João C. Fernandes [b,c], Eulália Pereira [a], Manuela E. Pintado [c], F. Xavier Malcata [c]

[a] *REQUIMTE, Departamento de Química, Faculdade de Ciências da Universidade do Porto, Rua do Campo Alegre, 4169-007 Porto, Portugal*
[b] *Departamento de Química, Faculdade de Ciências da Universidade do Porto, Rua do Campo Alegre, 4169-007 Porto, Portugal*
[c] *Escola Superior de Biotecnologia, Universidade Católica Portuguesa, Rua Dr. António Bernardino de Almeida, 4200-072 Porto, Portugal*

ARTICLE INFO

PACS:
82.35.Pq
87.64.Dz
62.20.−x

Keywords:
Atomic force microscopy
Chitosan
Antimicrobial
Chitooligosaccharides
Cell wall
Nanoindentation

ABSTRACT

Chitosan has been reported to be a non-toxic, biodegradable antibacterial agent. The aim of this work was to elucidate the relationship between the molecular weight of chitosan and its antimicrobial activity upon two model microorganisms, one Gram-positive (*Staphylococcus aureus*) and one Gram-negative (*Escherichia coli*). Atomic force microscopy (AFM) imaging was used to obtain high-resolution images of the effect of chitosans on the bacterial morphology. The AFM measurements were correlated with viable cell numbers, which show that the two species reacted differently to the high- and low-molecular-weight chitosan derivatives. The images obtained revealed not only the antibacterial effects, but also the response strategies used by the bacteria; cell wall collapse and morphological changes reflected cell death, whereas clustering of bacteria appeared to be associated with cell survival. In addition, nanoindentation experiments with the AFM revealed mechanical changes in the bacterial cell wall induced by the treatment. The nanoindentation results suggested that despite little modification observed in the Gram-positive bacteria in morphological studies, cell wall damage had indeed occurred, since cell wall stiffness was reduced after chitooligosaccharide treatment.

1. Introduction

Chitin is a natural polymer found in the exoskeletons of crustaceans and insects, and in the cell walls of certain fungi [1]. Full or partial deacetylation of this biopolymer produces chitosan, a linear-abundant polysaccharide, composed mainly of β-1,4 linked 2-deoxy-2-amino-D-glucopyranose and partially of β-1,4 linked 2-deoxy-2-acetamido-D-glucopyranose [2]. The biocompatibility and biodegradability of this polymer combined with its various biological properties such as antioxidative [3], antibacterial and antifungal effects [4–7], make it a promising candidate in a broad range of industrial and clinical applications. However, its high molecular weight (MW) causes poor solubility in acid-free aqueous media and has limited its application so far. Recent studies on chitosan have focused on reducing the polymer chain length, resulting in chitooligosaccharides (COS), which are not only water soluble [8] but also possess versatile functional properties such as antitumor activity [9] and enhancement of protective effects against infection by certain pathogens [10], including fungi and other microorganisms [6].

The antibacterial effect of chitosan seems to be closely related to its MW and degree of acetylation [11]. However, the results reported to date led to contradictory conclusions—some mentioned that chitosan is more effective in inhibiting growth of bacteria than COS [6,12–14], whereas others claimed that the higher MW chitosan leads, in some cases, to a decrease in its activity [15–17]. The mechanism via which different MW chitosans exert their antibacterial activity on different bacterial species has also generated inconsistent conclusions. The most widely mentioned hypotheses of formation of an impervious layer around the cell by chitosan or penetration of the bacteria cell wall by COS [13,16] are yet to be proven.

Atomic force microscopy (AFM) is a highly versatile microscopy technique that is particularly well suited to the study of microorganisms, because it combines a greatly improved resolution when compared to optical microscopy with little or no sample preparation required. In addition, compared to conventional scanning electron microscopy, samples may be studied in a more natural state, as there is no requirement to scan in vacuum or for a conductive coating. Therefore, AFM has been widely applied to studies of bacterial morphology [18–21]. While not suited to inspection of large samples and not capable of high throughput due to slow acquisition time, AFM can generate images ranging from tens of micrometers to tens of nanometers in size and hence has the resolution to image many bacteria at once,

* Corresponding author. Tel.: +351 22 040 2585; fax: +351 22 040 2659.
E-mail address: peter.eaton@fc.up.pt (P. Eaton).

0304-3991/$ - see front matter © 2008 Elsevier B.V. All rights reserved.
doi:10.1016/j.ultramic.2008.04.015

or to observe small changes in cell morphology, or even nanometer-scale features such as spore rodlets (3 nm in diameter) [22] or bacterial division septa [23,24].

Morphological applications of AFM to bacterial samples include imaging of pili, flagelli, etc. [19,25], genetic variation [24,26] and the study of antibacterial effects [24,27–29]. For example, the effect of the antibiotic vancomycin on the morphology of *Staphylococcus aureus* (*S. aureus*) has been studied by AFM [24]. The authors found no large differences in cell morphology on treatment, but did note changes in the appearance and number of the bacterial septa. On the other hand, treatment of *Escherichia coli* (*E. coli*) with the β-lactam antibiotic cefodizime [27] led to major changes in cell appearance. Compared to the standard rod-like morphology, after treatment with a low concentration of the antibiotic, the cells appeared to be fused end to end into long filament-like structures, but at high concentrations almost complete lysis of the cell occurred. Damage to *E. coli* cells caused by three different antimicrobial peptides has also been studied by AFM [28]; it was found that all studied peptides caused roughening of the cell surface and lesions in the cell wall, while one notably caused the formation of large lesions with leaking of fluid and vesicles from the interior of the cell.

In addition to imaging, it is also possible to measure the physical properties of the sample with AFM, because the probe and the sample are physically in contact. For example, adhesion forces [30], ligand–receptor binding [31,32] or mechanical properties [33–36] of the cell may be probed. Indentation or stiffness measurements are useful, because cell rigidity may be associated with intrinsic cell structure, turgor pressure [37], cell wall type or environmental factors such as treatment with antibacterial agents. For example, Beckmann et al. [34] found significant differences in cell rigidity between wild-type enteroaggregative *E. coli* and a mutant that did not produce dispersin, a protein thought to cover the cell wall. The difference in rigidity is presumably evidence that the protein does indeed coat the outside of the bacteria. In that work, only relative differences were measured in cell stiffness. However, it is also possible, at least in principle, to determine from nanoindentation measurements real physical parameters, such as cell stiffness, or Young's modulus (E) of the probed cells [36,38,39]. Such measurements are, however, affected by several factors. Firstly, the nature and shape of the probing tip should be well characterized and in general in AFM, while the nature of the tip material may be obtained from the manufacturer, the shape of the tip is not known for sure. The shape is often assumed to be within the limits described by the manufacturer, which may not be the case. In addition, the geometry of the tip is important for the most commonly used indentation model, usually known as the Hertzian model [29,40]. Commonly, the shape is assumed to be a sphere or a cone [29]. In addition, the non-perpendicular approach of the tip to the surface, and non-elastic response of the sample may complicate analysis. Ideally, the spring constant of the cantilever to which the tip is attached should also be determined in each case, as manufacturer's estimates are often incorrect [41], but the best method for this calibration is in itself a matter of debate. However, despite the specific assumptions involved in the analysis of nanoindentation data generated by AFM, there is general agreement between data produced by different authors: most whole bacteria exhibit a value of E of the order of 10^2–10^3 MPa [19]. Furthermore, as has been pointed out elsewhere, relative measurements are usually adequate for the cases studied [36]. In fact, A-Hassan et al. [33] have developed a technique called force integration to equal limits, which is quite qualitative, but clearly shows stiffness differences across cells, for example in the case of living canine kidney cells. This last described technique takes advantage of the lateral resolution of AFM to locally determine the stiffness on a nanoscale level. Other authors have used a similar technique to obtain nanoindentation maps across bacteria surfaces in order to visualize variation in stiffness across the cell [29].

This communication describes the application of AFM imaging to study the antimicrobial effect of chitosans and COS on *E. coli* and *S. aureus* as model Gram-negative and -positive organisms, respectively. The results are correlated with cell-viability studies, and help us to understand how the bacteria react to the treatment by the different polymers. In addition, nanoindentation of the bacterial cells is used to assess the effect of the COS on cell rigidity.

2. Experimental

2.1. Chitosans and microorganisms

Chitosan with an average MW 628 kDa (degree of deacetylation: 80–85%) was purchase from Sigma-Aldrich. Chitooligosaccharide mixture was purchased from Nicechem (Shanghai, China) with MW <3 kDa. For the preparation of the chitosan solution, as-received was dissolved in 1.0% (v/v) acetic acid to make a 2.5% (w/v)solution. Similarly, the COS as-received was dissolved in water to 2.5% (w/v). In both cases, the pH was adjusted to 5.8 with 10 M NaOH. After stirring overnight, the solutions were autoclaved at 120 °C for 15 min. Microorganisms were purchased from NCTC, *E. coli* (NCTC 9001) and *S. aureus* (NCTC 8532).

2.2. Assays for antibacterial activity

Antimicrobial activity of the two compounds was tested against the two strains in Muller–Hinton broth, using inocula of ca. 10^8–10^9 cell/mL. The solution of chitosan or COS was added to reach a final concentration of 0.50% (w/v). After fixed treatment times of 0, 2, 4 and 24 h of incubation at 37 °C, 1 mL of each sample was diluted and plated by the spread technique on plate count agar (Lab M). The plates were incubated at 37 °C for 24 h and the viable cell numbers were determined. Triplicate analyses of each sample were performed and each experiment was carried out in duplicate.

2.3. Preparation and analysis of AFM samples

The effect of the two compounds on the bacterial cell surfaces was examined by AFM. Samples were prepared by applying 40 μL of bacterial suspension without treatment (control) or treated with COS or chitosan onto a clean glass surface, followed by air-drying. The samples were incubated in the presence of COS or chitosan for the same treatment times as for the antibacterial assays. The samples were then gently rinsed with deionized water to remove salt crystals, and air dried again before analysis.

AFM was carried out with a Veeco Multimode IVa atomic force microscope (Veeco, Santa Barbara, CA), equipped with a j-type scanner (ca. $100 \times 100 \times 5\,\mu m^3$ scan range). Bacteria morphology studies were carried out in the tapping mode in air, using silicon cantilevers with a resonant frequency of approximately 150 kHz (MikroMasch, Tallinn, Estonia). Two independently produced samples were analyzed, and several different areas were studied on each sample, but only characteristic images are shown here. For nanoindentation experiments, the samples were first scanned in the tapping mode to identify suitable bacteria. In each case, cells that appeared to be intact were chosen for analysis. Nanoindentation was then performed in the contact mode, firstly on the glass slide surface, to calibrate the detector sensitivity, and

then in the center of the selected bacteria. The nanoindentation experiments were carried out with slightly stiffer tips (resonant frequency 310 kHz) of nominal spring constant 27 N/m, as these were found to be more sensitive to the treatment than the softer tips. An area within the center of each cell was selected for analysis and at least 25 force curves on each cell were measured. The data were averaged during analysis. Measurements were repeated with separately grown and treated bacteria and with a different AFM cantilever to check for reproducibility; however, all data presented here were generated with the same cantilever. Analysis of the curves on the basis of the Hertz model was carried out with PUNIAS software (P. Carl, P. Dalhaimer) [42], using the cone model of the tip, and the nominal spring constant.

3. Results and discussion

Morphological characterization of the control *E. coli* samples showed typically rod-shaped cells of 250–300 nm height and 1.6–2.5 μm length. Often the cells also showed many pili or fimbria, typically extended on the glass surface, but were also visible on the surface of the cell in some cases. The top image in Fig. 1 is a typical area showing three *E. coli* cells. Beckmann found that *E. coli* cells imaged in liquid had a significantly larger height as measured by AFM than those in air, presumably due to dehydration outside of the buffer solution [34]. However, it was also found that image quality, in terms of the level of detail observed on the cells, was considerably higher in air measurements. This was presumably due to the mobility of the outer lipopolysaccharide layer in liquid. In our case, the cells observed for the control sample were presumably somewhat dehydrated, but no lysis was observed. In fact, AFM analysis of 4-week-old samples showed that further dehydration had occurred, leading to a number of depressions in each cell and smaller cell height (160–280 nm), which leads us to suppose that the fresh samples were not completely dehydrated. Therefore, all the results shown here are from cells analyzed within 24 h of deposition.

Fig. 1 (left) shows images from samples treated with COS for 2, 4 and 24 h. The samples treated for 2 h showed few differences to the control bacteria. However, in the 4 h image, several differences are apparent. Firstly, the bacteria appeared in much larger clusters than previously. Secondly, some lysed cells could be seen, in the form of collapsed rods (an example is in the center of the cluster shown here). After 24 h the clusters observed were even larger, few small clusters and no isolated cells were observed. Within the clusters cells showed a rather different morphology, some appearing more spherical than rod-like, and the cells had a much rougher surface texture than untreated cells, or those treated for shorter times, similarly to the effect already described for antimicrobial peptides [28]. The portion of a large cluster presented in Fig. 1 shows some material surrounding the cluster in places, forming a layer: we suspect this could be intracellular

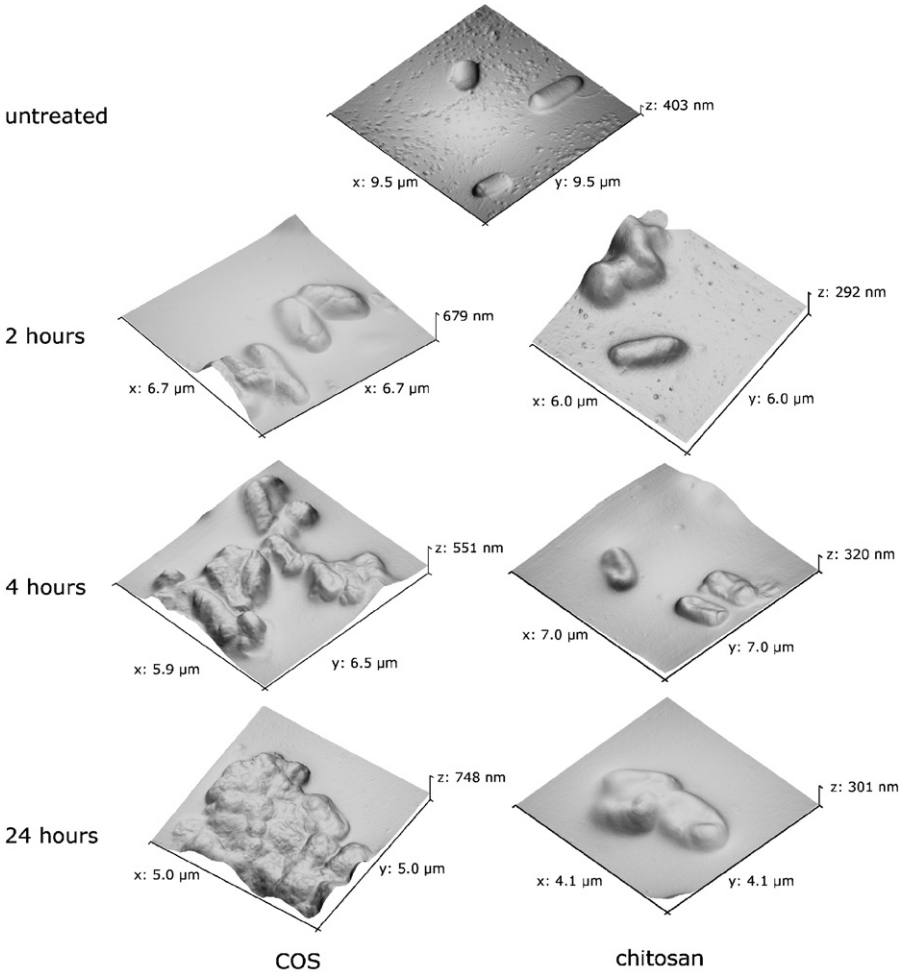

Fig. 1. AFM images of *E. coli*, before and after treatment with COS (left) and chitosan (right). The top image is of untreated bacteria, and below treatment times are as indicated in the image.

material visible after leakage or extracellular polymeric substance (EPS).

The images on the right of Fig. 1 show the response of the cells to chitosan. Rather like the response to COS, after 2 h little change was visible. After 4 h, the cells showed strong modifications in morphology. Many collapsed rods were seen in this sample, as shown in the figure. Unlike for the samples treated with COS, only small (<10 cell) clusters were seen, in which both intact and collapsed cells could be observed (data not shown). The abundant isolated rods were nearly always collapsed, indicating lysis of the cells. The 24 h sample was rather similar, exhibiting mostly isolated rods or small clusters; as shown, many cells had collapsed.

Fig. 2 shows the images of *S. aureus* before and after treatment. The top image shows part of a large cluster of cocci. It was found that the cells exist mostly in clusters in the native sample, and it was very rare to find isolated cells, which is a typical behavior for *S. aureus*. The sample showed the typical near-spherical shape of the cells (heights 300–700 nm), with some showing creases separating two halves of the cell, which may be observed in the image presented here. This feature has been identified as the septal plane of division, showing cells undergoing division [24]. The images on the left of the figure show the results of increasing treatment with COS. After 2 h, the cells appeared to be covered in a layer of the polymer, and were thus resolved less clearly. However, no gross morphological differences were seen. The main difference, as shown, was that the cells were more well-dispersed, with no large (>10 cocci) clusters observed, and some isolated cells were visible. After 4 h of treatment, the cells again existed mostly as small clusters or individual cells. At this time, some of the images showed what appeared to be damaged cells (see the two cells arrowed at the left of the image), with greatly roughened texture on the cell surface. However, most cells showed no significant morphological changes. After 24 h, as shown, the situation was very similar, with some small clusters, isolated cells, and the cell surfaces were rather uneven compared to the smooth surfaces of the untreated bacteria. The images on the right of Fig. 2 illustrate typical results after treatment with chitosan. The results after 2, 4 and 24 h were essentially identical. We found that the cells were even harder to resolve than with the COS, being covered in a thick layer of the polymer. Many isolated cells and only small clusters were observed for all treatment times. Interestingly, as seen in the image from 2 h treatment, some cells with the septa clearly visible were observed. Overall, the effect of the chitosan and COS on the cell morphology was much less intense in the case of *S. aureus* than for *E. coli*. This was somewhat expected, given the much thicker peptidoglycan layer of the cell wall of Gram-positive bacteria—which provides structural strength, and the absence of outer membrane [43,44]. However, it was not clear from the morphological studies alone whether the lack of visible changes meant that less damage was caused to the cells or if it only meant that due to greater mechanical resistance the cells exhibited less morphological change after chitosan or COS action.

In order to clarify these results, it was decided to carry out nanoindentation studies on the treated and untreated bacteria to

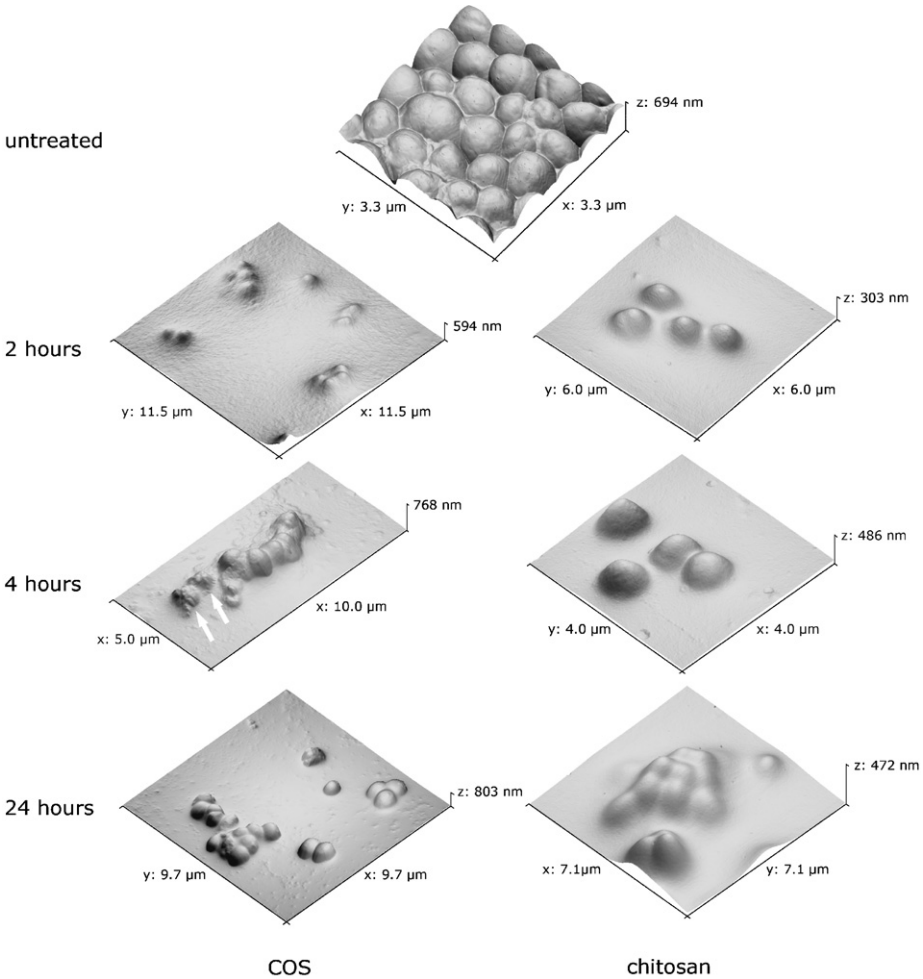

Fig. 2. AFM images of *S. aureus,* before and after treatment with COS (left) and chitosan (right). The top image is of untreated bacteria, and below treatment times are as indicated in the image. Arrows show specific cells referred to in the text.

ascertain if the polymer treatment affected the mechanical strength of the cells. As described in the introduction, this technique can give stiffness measurements of the surface of individual cells, which can be sensitive to treatment, and the bacterial strain [34,38,45]. Cells which appeared intact were selected, in order to assess any treatment effects even where morphological studies showed no change. Care was taken to ensure that all measurements were made within the center of the cell, however, as it is known that geometric effects can change the measured stiffness when comparing edges to the center of the cell [18,35]. Data were later averaged for analysis. High-resolution images of the treated bacterial cell surfaces revealed a typical chitosan-like texture on the chitosan-treated cells; however, the COS-treated cell surfaces did not reveal the presence of the remaining compound. Attempts to remove the polymer film by washing were unsuccessful. Therefore, it was decided to study only the bacteria treated by COS by this technique, as nanoindentation on cells coated with chitosan might probe the polymer rather than the bacteria. Untreated bacteria were studied as a control and compared to bacteria treated for 4 h, as the morphological studies showed clear effects after this time. Typical raw deflection data from the nanoindentation experiments are shown for both *E. coli* and *S. aureus* in Fig. 3, along with reference curves obtained on glass. Firstly, it may be seen that in all cases the slopes for the bacteria curves were less steep than for the glass, showing that indentation or compression of the cells had occurred. Secondly, it may be observed that for both *E. coli* and *S. aureus*, the bacteria treated with COS exhibited lower slopes than for the untreated bacteria. Therefore the cells were considerably less stiff after treatment. This presumably reflects cell wall weakening, either by cell wall damage alone or accompanied by some lysis of the cell. As described above, averaged nanoindentation data and the Hertzian mechanics model were used to obtain values of Young's modulus (E) for the two types of bacteria studied. The results are presented in Table 1. Once again, the data indicate that in both cases, the treatment with the COS reduced the stiffness of the cells. This reduction was slightly greater for *E. coli* than for *S. aureus*, both in absolute and relative terms (the *E. coli* stiffness was reduced to 82% of the untreated cell's value on average, while for *S. aureus* it was 92%).

Comparing the data of these two species, we were surprised to see that *S. aureus* appeared less resistant to the AFM tip than *E. coli. S. aureus* is a Gram-positive species—the peptidoglycan layer is substantially thicker in Gram-positive bacteria (20–80 nm) than in -negative bacteria (7–8 nm). The function of the peptidoglycan is to give shape and strength to the cell wall. However, although the Gram-negative *E. coli* has a much thinner layer of peptidoglycan, it possesses an additional layer, the outer membrane [43,44].

Despite a large number of studies of nanoindentation on bacteria (see Ref. [19] for a review), some of which report values of E [29,38], we could not find any comparisons between stiffness of Gram-positive and -negative bacteria. However, we repeated the experiments with an independently grown and treated set of bacteria and a different cantilever, and the trend in the results was the same; suggesting that for these particular stains of bacteria, the *S. aureus* is indeed of lower stiffness than the *E. coli*. Another possibility is that the results are an artifact of the experiment, caused by the different geometries of the two species (cocci and rod-shaped).

It is instructive to compare the data obtained from the AFM experiments already described, to those obtained by standard cell-counting studies. The results of cell-viability studies on the two bacteria, using both COS and chitosan are presented in Fig. 4. It may be seen that the trend in the results differs for the two organisms, and also for the two compounds studied, which are

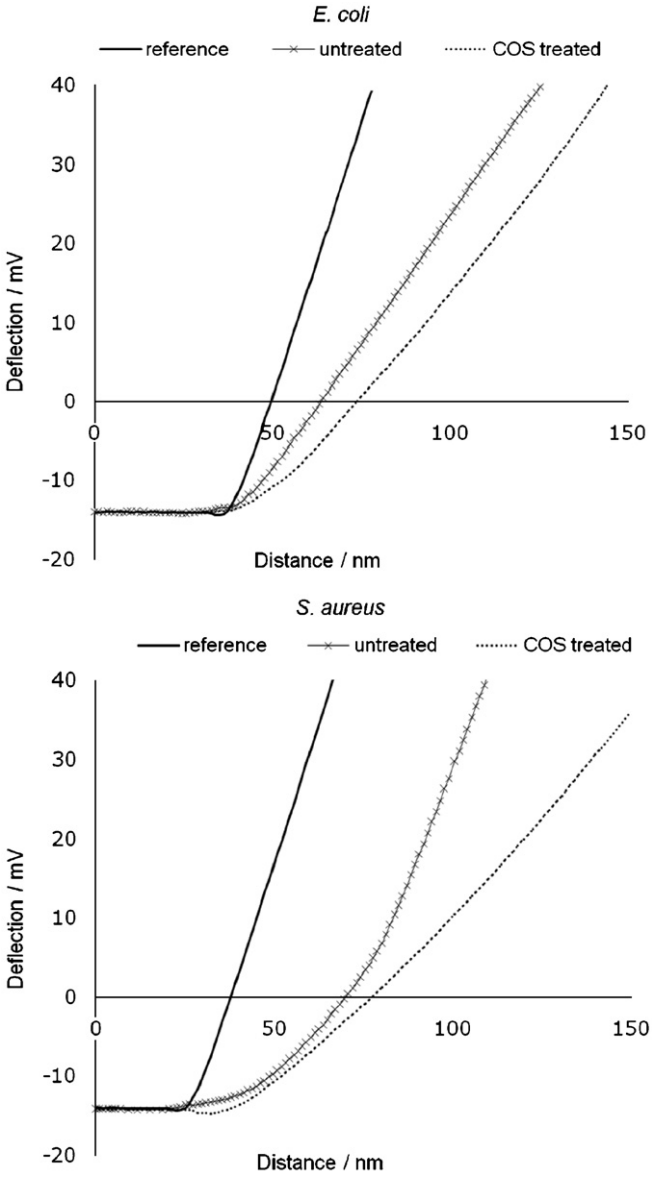

Fig. 3. Raw nanoindentation data for the two species before and after treatment with chitooligosaccharide (COS) for 4 h. The reference curve shown was used as a sensitivity calibration. Typical curves are shown.

Table 1
Results of Hertzian mechanics fitting to mean nanoindentation curves measured on untreated (control) bacteria or bacteria treated for 4 h with chitooligosaccharide (COS)

	E. coli control E (MPa)	*E. coli* COS E (MPa)	*S. aureus* control E (MPa)	*S. aureus* COS E (MPa)
Mean	221.4	182.2	95.4	88.2
Standard deviation	11.9	14.4	2.6	5.5

themselves only different in terms of their MWs. In the case of *E. coli*, the COS acted very quickly to reduce the number of viable cells by almost three orders of magnitude within the first 4 h. However, between 4 and 24 h the number of viable cells showed no further reduction. In the case of the chitosan, however, while the initial reduction in cell viability was slower, over the 24 h, a greater reduction was achieved. Further data (not shown) confirm these results as after 48 h the low-MW COS-treated population

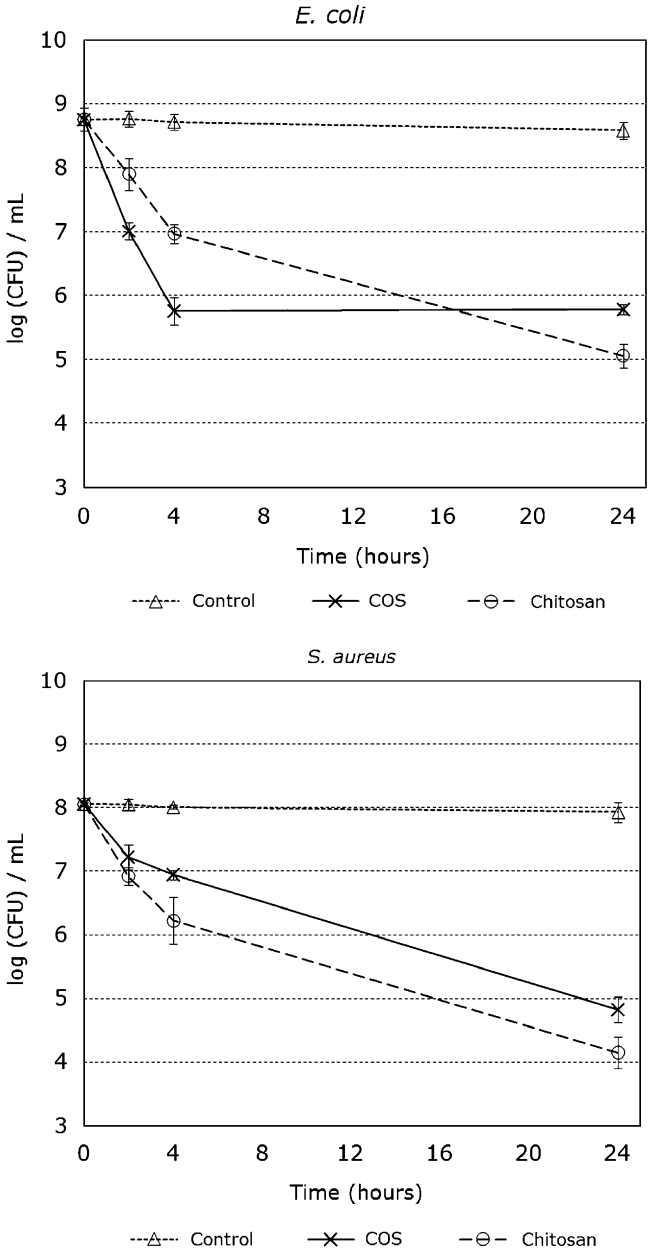

Fig. 4. Enumeration of viable cell numbers (colony forming units—CFUs) for *S. aureus* and *E. coli* treated with chitooligosaccharide (COS) or chitosan, through 24 h. Error bars represent the standard deviations.

actually increased slightly, whereas the higher-MW chitosan continued to further reduce the number of viable cells. Comparing these data to the AFM allows us to understand the mode of action more clearly. In the case of the low-MW COS, the *E. coli* responded to the treatment by clustering probably due to the ionic interaction between COS and cell wall (since COS is in the protonated form under the pH conditions used) or due to the production of EPS. This presumably protected the bacteria in the interior of the clusters from the action of the COS, preventing further bacterial population reduction after 4 h of treatment time. However, for the high-MW chitosan the polymer prevented this clustering mechanism (possibly due to comparatively lower ionic influence versus the COS); hence, many more isolated bacteria were observed, and also more evidence was seen of cell death (collapsed rods). We may also postulate that the polymer coating the cells observed in many cases for the chitosan interfered with the communication between the cells, further hampering their defenses. According to the cell-viability studies, the action of the chitosan was slower, but the antibacterial effect was maintained for longer (stronger bactericidal than bacteriostatic effect), resulting in a greater effect in the long term.

Looking at the results from *S. aureus*, the trends in the action of the two polymers were rather similar. For both polymers, the initial treatment caused a rapid decrease in the number of viable cells, which continued throughout the period of study. The only difference was that for all treatment times, the high-MW chitosan killed more cells than the low-MW COS. Based on the AFM images, it might be surmised that the high-MW chitosan surrounds the cocci preventing absorption of nutrients, and the normal function of the cells, therefore increasing the efficiency of the treatment. Our results suggested that the antimicrobial effect is strongly dependent on the type of target microorganism and the MW of chitosan—being higher for lower MW in the case of the Gram-negative bacterium tested, and the opposite holding in the case of the Gram-positive bacterium. Zheng and Zhu suggested that the different action upon Gram-positive and -negative microorganisms is likely to be due to the intrinsic difference in cell wall structure—it being easier for oligomers to penetrate the Gram-negative cell wall. In their Gram-positive counterparts, a mechanical barrier is formed by higher-MW chitosans, which prevents nutrient absorption [16]. Liu and his co-workers showed, using a confocal laser scanning microscope, that chitosan oligomers actually penetrate *E. coli*, suggesting that its antibacterial activity seemed to be mainly caused by the inhibition of the DNA transcription [15].

4. Conclusion

Use of AFM imaging studies helped us to understand how chitosans with different MWs act differently on model Gram-positive and -negative bacteria. Specifically, cell lysis, surface roughening and cell clustering were observed. In the case of *E. coli*, the apparent response strategy used by the bacterium, forming large clusters means the low-MW COS had only a short-lived effect on the cell-viability—i.e. a bacteriostatic effect. On the other hand, the high-MW chitosan prevented this behavior, and consequently was a more effective antibacterial agent. *S. aureus* exhibited less morphological change on treatment, but nanoindentation studies revealed that even so the cells were weakened by treatment with the COS, which confirms the cell viability studies. Our results showed that the antimicrobial effect is strongly dependent on the target microorganism and the MW of chitosan—we saw stronger antimicrobial effects for lower MW in the case of the Gram-negative bacterium tested, and the opposite in the case of the Gram-positive bacterium.

Acknowledgments

The authors gratefully acknowledge Dr. Maria Feio for helpful discussions, and Dr. Phillipe Carl for help with the PUNIAS software. João C. Fernandes thanks the FCT for fellowship (SFRH/BD/31087/2006) funded by the POCI2010 program, with the support the European Union.

References

[1] M. Rinaudo, Prog. Polym. Sci. 31 (7) (2006) 603.
[2] C.L. Vernazza, G.R. Gibson, R.A. Rastal, Carbohydr. Polym. 60 (4) (2005) 539.
[3] P.-J. Chien, F. Sheu, W.-T. Huang, M.-S. Su, Food Chem. 102 (4) (2007) 1192.
[4] N. Liu, X.G. Chen, H.J. Park, C.G. Liu, C.S. Liu, X.H. Meng, L.J. Yu, Carbohydr. Polym. 64 (1) (2006) 60.

[5] V.E. Tikhonov, E.A. Stepnova, V.G. Babak, I.A. Yamskov, J. Palma-Guerrero, H.-B. Jansson, L.V. Lopez-Llorca, J. Salinas, D.V. Gerasimenko, I.D. Avdienko, V.P. Varlamov, Carbohydr. Polym. 2006 (1) (2006) 66.
[6] Y. Uchida, M. Izume, A. Ohtakara, in: G. Skjåk-Bræk, T. Anthonsen, P. Sandford (Eds.), Chitin and Chitosan: Sources, Chemistry, Biochemistry, Physical Properties and Applications, Elsevier, London, UK, 1989, p. 373.
[7] J. Rhoades, S. Roller, Appl. Environ. Microbiol. 66 (1) (2000) 80.
[8] S.-K. Kim, N. Rajapakse, Carbohydr. Polym. 62 (4) (2005) 357.
[9] K. Tsukada, T. Matsumoto, K. Aizawa, A. Tokoro, R. Naruse, S. Suzuki, M. Suzuki, Japan. J. Cancer res.: Gann 81 (3) (1990) 259.
[10] K. Suzuki, T. Mikami, Y. Okawa, A. Tokoro, S. Suzuki, M. Suzuki, Carbohydr. Res. 151 (1986) 403.
[11] H.W. Lee, Y.S. Park, J.S. Jung, W.S. Shin, Anaerobe 8 (6) (2002) 319.
[12] F. Shahidi, J.K.V. Arachchi, Y.J. Jeon, Trends Food Sci. Technol. 10 (2) (1999) 37.
[13] C. Qin, H. Li, Q. Xiao, Y. Liu, J. Zhu, Y. Du, Carbohydr. Polym. 63 (3) (2006) 367.
[14] Y.-J. Jeon, P.-J. Park, S.-K. Kim, Carbohydr. Polym. 44 (1) (2001) 71.
[15] X.F. Liu, Y.L. Guan, D.Z. Yang, Z. Li, K.D. Yao, J. Appl. Polym. Sci. 79 (7) (2001) 1324.
[16] L.-Y. Zheng, J.-F. Zhu, Carbohydr. Polym. 54 (4) (2003) 527.
[17] X.-K. Wei, C.-L. Lei, Agric. Sci. China 3 (4) (2004) 299.
[18] C.J. Wright, I. Armstrong, Surf. Interface Anal. 38 (11) (2006) 1419.
[19] A.V. Bolshakova, O.I. Kiselyova, I.V. Yaminsky, Biotechnol. Prog. 20 (6) (2004) 1615.
[20] A.V. Bolshakova, O.I. Kiselyova, A.S. Filonov, O.Y. Frolova, Y.L. Lyubchenko, I.V. Yaminsky, Ultramicroscopy 86 (1–2) (2001) 121.
[21] M.J. Doktycz, C.J. Sullivan, P.R. Hoyt, D.A. Pelletier, S. Wu, D.P. Allison, Ultramicroscopy 97 (1–4) (2003) 209.
[22] L.M. Zhao, D. Schaefer, M.R. Marten, Appl. Environ. Microbiol. 71 (2) (2005) 955.
[23] A. Touhami, M.H. Jericho, T.J. Beveridge, J. Bacteriol. 186 (11) (2004) 3286.
[24] S. Boyle-Vavra, J. Hahm, S.J. Sibener, R.S. Daum, Antimicrob. Agents Chemother. 44 (12) (2000) 3456.
[25] A. da Silva, O. Teschke, World J. Microbiol. Biotechnol. 21 (6–7) (2005) 1103.
[26] S.E. Cross, J. Kreth, L. Zhu, F.X. Qi, A.E. Pelling, W.Y. Shi, J.K. Gimzewski, Nanotechnology 17 (4) (2006) S1.
[27] P.C. Braga, D. Ricci, Antimicrob. Agents Chemother. 42 (1) (1998) 18.
[28] M. Meincken, D.L. Holroyd, M. Rautenbach, Antimicrob. Agents Chemother. 49 (10) (2005) 4085.
[29] I.B. Beech, J.R. Smith, A.A. Steele, I. Penegar, S.A. Campbell, Colloids Surfac. B—Biointerfaces 23 (2–3) (2002) 231.
[30] Y.F. Dufrene, Micron 32 (2) (2001) 153.
[31] M. Gad, A. Itoh, A. Ikai, Cell Biol. Int. 21 (11) (1997) 697.
[32] V. Dupres, F.D. Menozzi, C. Locht, B.H. Clare, N.L. Abbott, S. Cuenot, C. Bompard, D. Raze, Y.F. Dufrene, Nat. Methods 2 (7) (2005) 515.
[33] E. A-Hassan, W.F. Heinz, M.D. Antonik, N.P. D'costa, S. Nageswaran, C.A. Schoenenberger, J.H. Hoh, Biophys. J. 74 (3) (1998) 1564.
[34] M.A. Beckmann, S. Venkataraman, M.J. Doktycz, J.P. Nataro, C.J. Sullivan, J.L. Morrell-Falvey, D.P. Allison, Ultramicroscopy 106 (8–9) (2006) 695.
[35] S.B. Velegol, B.E. Logan, Langmuir 18 (13) (2002) 5256.
[36] A. Vinckier, G. Semenza, Febs Lett. 430 (1998) 12.
[37] M. Arnoldi, M. Fritz, E. Bauerlein, M. Radmacher, E. Sackmann, A. Boulbitch, Phys. Rev. E 62 (1) (2000) 1034.
[38] J. Wang, S. He, S. Xie, L. Xu, N. Gu, Mater. Lett. 61 (3) (2007) 917.
[39] W.R. Bowen, R.W. Lovitt, C.J. Wright, Biotechnol. Lett. 22 (11) (2000) 893.
[40] M. Heuberger, G. Dietler, L. Schlapbach, Nanotechnology 6 (1) (1995) 12.
[41] G.A. Matei, E.J. Thoreson, J.R. Pratt, D.B. Newell, N.A. Burnham, Rev. Sci. Instrum. 77 (8) (2006) 083703.
[42] P. Carl, C.H. Kwok, G. Manderson, D.W. Speicher, D.E. Discher, Proc. Nat. Acad. Sci. USA 98 (4) (2001) 1565.
[43] M.R.J. Salton, K.S. Kim, Baron's Medical Microbiology, University of Texas Medical Branch, Austin, TX, 1996.
[44] M. Madigan, J. Martinko, Brock Biology of Microorganisms, Prentice-Hall, New Jersey, 2005.
[45] I. Penegar, C. Toque, S.D.A. Connell, J.R. Smith, S.A. Campbell, in: Additional Papers from the 10th International Congress on Marine Corrosion and Fouling, 2001.